Relationships between net photosynthesis and steady-state chlorophyll fluorescence retrieved from airborne hyperspectral imagery

CrossMark

P.J. Zarco-Tejada [a],[*], A. Catalina [b], M.R. González [b], P. Martín [b]

[a] Instituto de Agricultura Sostenible (IAS), Consejo Superior de Investigaciones Científicas (CSIC), Córdoba, Spain
[b] Departamento de Producción Vegetal y Recursos Forestales, ETS de Ingenierías Agrarias, Universidad de Valladolid, Palencia, Spain

ARTICLE INFO

ABSTRACT

Previous studies have demonstrated the link between leaf chlorophyll fluorescence and photosynthesis, mainly at the leaf level and under controlled laboratory conditions. The present study makes progress in demonstrating the relationship between steady-state fluorescence and net photosynthesis measured under natural light field conditions both at the leaf and image levels. Ground measurements and airborne campaigns were conducted over two summers to acquire hyperspectral imagery at 40 cm resolution and 260 spectral bands in the 400–885 nm spectral region. This enabled the identification of pure vegetation pixels to extract their radiance spectra. The datasets were collected in August 2010 and 2011 in the western part of the area included in the Ribera del Duero Designation of Origin (*Denominación de Origen*), in northern Spain. The experiments were conducted in twelve full production vineyards where two study plots per field were selected to ensure adequate variability in leaf biochemistry and physiological condition. The vineyard fields were selected on the basis of their gradient in leaf nutrition and plant water status and showed variability in leaf pigment values and stomatal conductance. Leaves were collected for destructive sampling and biochemical determination of chlorophyll $a + b$, carotenoids and anthocyanins in the laboratory. Leaf steady-state and dark-adapted fluorescence parameters, net photosynthesis (P_n) and stomatal conductance (G_s) were measured in the field under natural light conditions. Such data were used as a validation dataset to assess fluorescence–photosynthesis relationships both at the leaf and the image level. The Fraunhofer Line Depth (FLD) principle based on three spectral bands (FLD3) was the method used to quantify fluorescence emission from radiance spectra extracted from pure vegetation pixels identified in the hyperspectral imagery. Fluorescence retrievals conducted using the FLD3 method yielded significant results when compared to ground-measured steady-state F_s ($r^2 = 0.48$; $p < 0.01$) and F_v'/F_m' ($r^2 = 0.53$; $p < 0.01$). The two-year assessment yielded consistent results on the relationship between P_n and F_s both at the leaf level and based on the airborne hyperspectral imagery. At the leaf level, significant relationships were found between leaf F_s and P_n ($r^2 = 0.55$; $p < 0.001$ for 2010; $r^2 = 0.59$; $p < 0.001$ for 2011). At the hyperspectral image level, the agreement between leaf P_n and airborne F was consistent for both years separately, yielding significant relationships at $p < 0.01$ for 2010 ($r^2 = 0.54$) and 2011 ($r^2 = 0.41$) and a significant relationship at $p < 0.001$ for the aggregated years ($r^2 = 0.52$). Results show the link between net photosynthesis and steady-state fluorescence obtained under natural sunlight conditions at both leaf and airborne hyperspectral imagery levels.

1. Introduction

A number of studies have demonstrated the link between leaf chlorophyll fluorescence and photosynthesis (Krause & Weis, 1984; Larcher, 1994; Lichtenthaler, 1992; Lichtenthaler & Rinderle, 1988; Papageorgiou, 1975; Schreiber & Bilger, 1987; Schreiber et al., 1994). In particular, experiments conducted at the leaf and laboratory level in controlled environments have shown that fluorescence and reflectance indices were able to track diurnal changes caused by heat and water stress (Dobrowski et al., 2005). Under water deficit conditions, red edge indices measured at the canopy level have shown sensitivity to temperature and stress through steady-state fluorescence (F_s), tracking CO_2 assimilation. Such findings confirm earlier results obtained at the leaf level by a study comparing fluorescence and net photosynthesis relationships at the leaf level under water stress in grapevines (Flexas et al., 2000). In that study, leaf measurements showed a link between gas-exchange rates of CO_2, H_2O and chlorophyll fluorescence data.

* Corresponding author at: Instituto de Agricultura Sostenible (IAS), Consejo Superior de Investigaciones Científicas (CSIC), Alameda del Obispo, s/n, 14004—Córdoba, Spain. Tel.: +34 957 499 280, +34 676 954 937; fax: +34 957 499 252.
E-mail address: pablo.zarco@csic.es (P.J. Zarco-Tejada).
URL: http://quantalab.ias.csic.es (P.J. Zarco-Tejada).

Although such studies have clearly shown the interest of monitoring chlorophyll fluorescence as an indicator of photosynthesis, several earlier studies focused instead on the Photochemical (or Physiological) Reflectance Index (PRI) (Gamon et al., 1992) as a proxy for photosynthesis. In particular, they evaluated the potential for measuring terrestrial photosynthesis from space (Grace et al., 2007) using reflectance (PRI) and fluorescence (F) indices. Specific assessments of the dynamic changes in chlorophyll fluorescence vs. the PRI and photosynthesis were conducted in grapevines (Evain et al., 2004), Scots pine (Louis et al., 2005), experimental mangrove canopies (Nichol et al., 2006) and coastal shrubs (Naumann et al., 2008). In natural vegetation developed under salt and drought stress, both dark-adapted and steady-state chlorophyll fluorescence measures were used to detect effects on physiology before they were evident (Naumann et al., 2007).

Despite the successful results obtained in some cases with the PRI as a proxy for photosynthesis, some studies have shown that this index is highly affected by the canopy structure, leaf pigments and background (Suárez et al., 2008, 2009). In fact, this can prevent the successful monitoring of photosynthesis (Rascher & Pieruschka, 2008). In this latter study, the PRI failed to monitor photosynthetic light conversion due to the effects of the canopy structure on the index, suggesting the use of fluorescence as a better indicator of photosynthesis. The modeling study conducted by Zarco-Tejada et al. (2009) showed that fluorescence estimations using *in-filling* methods were little affected by structural changes of the canopy such as leaf area density. On the other hand, other *standard* indicators suggested in the past for canopy monitoring such as the NDVI or leaf chlorophyll content are highly affected by the canopy medium and fail to track photosynthesis (Stylinski et al., 2002). This confirms the need for sensitive indices related to short-term physiological changes.

In recent years, increasing attention has been given to chlorophyll fluorescence for global monitoring of vegetation physiology. Specific studies have explored the technical aspects and challenges of retrieving fluorescence to monitor global photosynthesis (Malenovsky et al., 2009). They have discussed scaling issues from the leaf to the region level using O_2 bands for fluorescence quantification (Rascher et al., 2009) and modeled gross primary production (GPP) from fluorescence/assimilation rates in diurnal patterns (Damm et al., 2010). These efforts related to global photosynthesis mapping through fluorescence quantification have received much attention as part of the FLuorescence EXplorer FLEX mission (FLEX) supported by the European Space Agency (ESA) Earth Explorer program. Under such scope, earlier modeling work was conducted as part of the Vegetation Fluorescence Canopy Model (FluorMOD project) (Miller et al., 2004), which served to develop a leaf model named FluorMODleaf (Pedrós et al., 2004, 2008, 2010) and a canopy model named FluorSAIL (Verhoef, 2004). These models were used as a first tool to explore the feasibility of retrieving the fluorescence signal superimposed on the leaf and canopy reflectance spectra. These earlier efforts were critical for the simulation work conducted later to assess F retrieval accuracy in response to relevant sensor properties, including the spectral sampling interval, spectral resolution, signal to noise and spectral shift, along with different fluorescence retrieval methods (Damm et al., 2011). These experimental and modeling advances enabled the development of SCOPE (Van der Tol et al., 2009a,b), an integrated leaf-canopy fluorescence-temperature-photosynthesis model. The abovementioned modeling studies are critical to understand the feasibility of fluorescence retrieval at both leaf and canopy levels. They have shown that it is a challenging task since the contribution to the radiance signal is estimated to be about 2–3%. Thanks to these efforts, several methods have been reported to extract the fluorescence signal at the leaf and canopy levels with very narrow spectral bands (Meroni et al., 2004, 2008a,b, 2009; Moya et al., 2004; Pérez-Priego et al., 2005), proving the feasibility of fluorescence retrieval using the O_2-A band feature. Recently, global maps of chlorophyll fluorescence have been published (Frankenberg et al., 2011; Joiner et al., 2011) using the Thermal And Near infrared Sensor for carbon Observation sensor (TANSO) on board GOSAT (Kuze et al.,

2009). The fluorescence retrievals and global maps obtained from GOSAT were discussed by Guanter et al. (2012), who found overall good agreement between fluorescence quantification by the satellite sensor and annual and seasonal patterns of vegetation.

Although these recent advances in the global mapping of fluorescence are a major step forward, progress in leaf-canopy fluorescence modeling and near-field validation experiments is critical to understand the fluorescence signal linked to photosynthesis under natural sunlight conditions in pure vegetation pixels. This is particularly important as vegetation structure, background, illumination and atmospheric effects play a critical role at larger scales where the fluorescence signal is quantified in mixed pixels that aggregates shadows, pure vegetation and the background. Few published validation studies have addressed the retrieval of fluorescence at the image level and the relationships between fluorescence retrieved and field-measured photosynthesis under natural light conditions. This is due to the lack of appropriate imagery acquired at high spatial and spectral resolutions and the complexity of the field validation required. Recent studies (Zarco-Tejada et al., 2009) applying the *in-filling* method to 1 nm FWHM airborne multispectral imagery acquired over crops for stress detection have shown the feasibility of mapping fluorescence at 40 cm resolution using a micro-hyperspectral imager on board an unmanned aerial vehicle (UAV) (Zarco-Tejada et al., 2012).

Despite the improvements in high-resolution fluorescence retrieval from pure vegetation pixels under varying physiological conditions, studies focused on the link between fluorescence quantification from high-resolution imagery and field photosynthesis data are still lacking. In the present study, field photosynthesis and fluorescence data and high-resolution airborne hyperspectral imagery were collected over two summers. The aim was to explore the relationships between fluorescence, pigment content and net photosynthesis in pure vegetation pixels extracted from the imagery. Leaf and canopy level fluorescence and hyperspectral radiance images were used to explore i) the relationships between leaf fluorescence measures and photosynthesis data during two consecutive years, assessing steady-state and dark-adapted fluorescence parameters as well as leaf chlorophyll, carotenoid and anthocyanin pigment data; and ii) the link between airborne F quantification extracted from pure vegetation pixels and photosynthesis data in a validation study conducted over two summers.

2. Materials and methods

2.1. Field experiments and airborne campaigns

2.1.1. Study site description

The study was conducted in 2010 and 2011 in the western part of the area included in the Ribera del Duero Designation of Origin (*Denominación de Origen*), in Peñafiel, Valladolid, northern Spain, at an altitude of 800 m above sea level. A group of non-irrigated full production vineyards were selected to ensure adequate variability in soil background and physiological status according to the purposes of the study. This resulted in 24 different 10 × 10 m study plots. All the vineyards had been planted between 1983 and 1994 with cv. Tempranillo grafted on 110-Richter rootstock. The vines, spaced 3 × 1.5 m apart, were trained to double cordons and spur pruned, with an average bud count of 16 buds per plant. Shoots were maintained in a vertical position (trellis). The main wire was 0.70 m above the soil surface.

Soils were calcareous (up to 58.8% total carbonate content) and poor in organic matter (about 0.76%), with an average pH of 8.6. Texture ranged from medium to medium-weighted. Concentrations of active carbonate (3.3–15.5%) and DPTA extractable iron (2.3–6.4 mg kg^{-1}) were highly heterogeneous within the area. Such soil properties along with the presence of a sensitive rootstock (110-Richter) led to different levels of iron deficiency chlorosis in the vineyards of the area. The study plots had high variability of soil concentrations of extractable potassium (86–345 mg kg^{-1}), phosphorus (4.6–31.8 mg kg^{-1}) and magnesium (120–663 mg kg^{-1}). The area has Mediterranean climate, with low

temperatures in winter and hot and dry summers. Mean annual temperatures in the study area were 11.2 °C and 12.2 °C in 2010 and 2011, respectively. The rainfall registered was only 414 mm in the first year and 286 mm in the second one. Without irrigation, these insufficient water supplies in soils varying in texture and root explorable depth ensured a broad variability of water status levels in the study zones.

2.1.2. Field data collection

Simultaneous measurements of leaf gas exchange and chlorophyll fluorescence parameters were taken at veraison under field conditions, coinciding with the airborne campaigns (24–25 August in 2010 and 17–18 August in 2011). Gas exchange (net assimilation, P_n, and stomatal conductance, G_s) and chlorophyll fluorescence parameters were monitored using a LI-Cor 6400 portable infrared gas analyzer (IRGA) equipped with a 6400–40 leaf chamber pulse amplitude modulation (PAM) fluorometer (Li-Cor, Inc. Lincoln, Nebr., USA). Fluorescence parameters included minimum (F_o) and maximum (F_m) fluorescence in dark-adapted leaves (F_o' and F_m' under light conditions), variable (F_v) and steady-state fluorescence (F_s), efficiency (ΦPSII) and maximum efficiency (F_v/F_m and F_v'/F_m') of photosystem II, apparent rate of electron transport (ETR) and photochemical (qP) and non-photochemical quenching (NPQ).

Nine fully expanded leaves exposed to direct solar radiation and inserted at the fourth or fifth node from the apex were selected in each study plot to conduct the photosynthesis measurements. Chlorophyll fluorescence parameters of dark-adapted leaves were obtained before dawn (1:00–3:00 h local time), while levels of gas exchange and chlorophyll fluorescence of light-adapted leaves were obtained at midday (11:00–13:00 h local time). The leaves obtained from each site were used to determine assimilation and fluorescence levels, and to ensure that field measurements were coincident with the airborne campaigns. Only nine leaves per plot were selected for measurement, as a larger number would have caused longer time gaps between the airborne overpasses and the field measurements conducted. Leaf chamber conditions were set constant for all measurements conducted: incident photosynthetic photon flux density (PPFD) on the leaves was set to 1500 µmol photons $m^{-2} s^{-1}$, which is known to be above

photosynthetic saturation in field-grown grapevines (Escalona et al., 1999; Flexas et al., 1998); CO_2 levels in the analyzer were held constant at 370 µmol CO_2 mol^{-1} air. Temperature, air pressure and relative humidity were maintained at ambient levels. Air flow rate through the leaf chamber was maintained at 500 µmol s^{-1}. Leaf absorbances measured at 635 nm and 465 nm were entered in the IRGA for photosynthetic measurements conducted in each study site. These values were estimated from leaf greenness data previously obtained with a CL-01 portable colorimeter (Hansatech Instruments Ltd., Norfolk, UK), as described by González et al. (2005). At veraison, twenty expanded leaves were sampled from the top of the canopy in each study plot for biochemical determination of foliar pigments in the laboratory (see details of the protocols used in Zarco-Tejada et al. (2005) and Steele et al. (2009)). Chlorophyll a (C_a), chlorophyll b (C_b) and total carotenoid (C_{xc}) concentrations were calculated using the extinction coefficients derived by Lichtenthaler (1987) with absorbance measured at 470 nm, 645 nm and 662 nm. Anthocyanin content was determined from extract absorbance at 530 nm (Steele et al., 2009), with an anthocyanin absorption coefficient as in Strack and Wray (1989). All pigment content data were expressed on a leaf area basis.

2.1.3. Airborne campaigns

Airborne campaigns were conducted in 2010 and 2011 using a micro-hyperspectral imager on board unmanned aerial vehicles (UAV) operated by the Laboratory for Research Methods in Quantitative Remote Sensing (QuantaLab, IAS-CSIC, Spain) (Berni et al., 2009; Zarco-Tejada et al., 2008, 2012). The UAV platforms used were designed to carry thermal, multispectral and hyperspectral imaging sensors. Two UAV platforms of different size, wingspan and payload capacity were used to successfully accomplish the airborne campaigns. The UAV platform operated in 2010 was a 2-m wingspan fixed-wing platform with up to 1-hour endurance at 5.8 kg take-off weight (TOW) and 63 km/h ground speed (mX-SIGHT, UAV Services and Systems, Germany). Due to the additional weight required to carry the micro-hyperspectral imager, the platform was operated at 6.3 kg TOW with reduced battery capacity, yielding 20-minute endurance only. Due to this limited endurance when carrying the hyperspectral imager, a larger UAV platform was developed for hyperspectral imagery acquisition. It was a 5-m
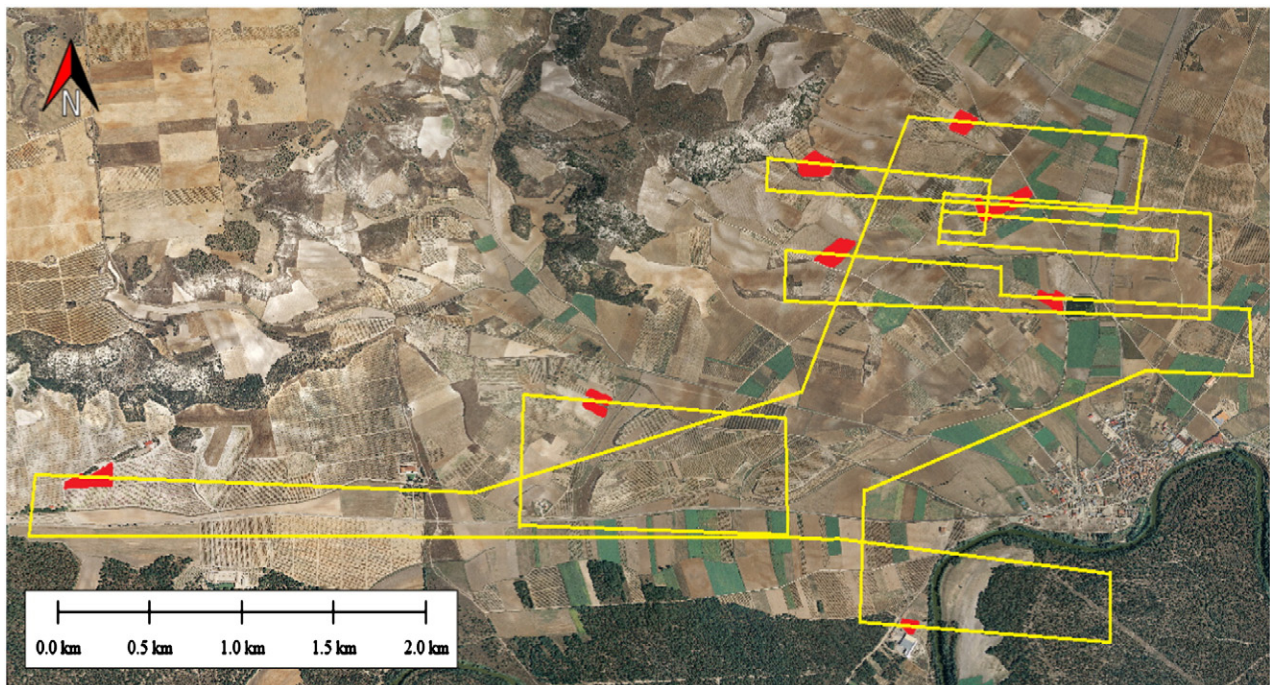

Fig. 1. Flight plan conducted in the 2010 and 2011 airborne campaigns by the unmanned aerial vehicle carrying the micro-hyperspectral imager. The study fields where leaf validation data were acquired are shown in red. Background image: IGN, PNOA, 2010.

wingspan fixed-wing platform with up to 3-hour endurance at 13.5 kg TOW and 66 km/h ground speed (Viewer, ELIMCO, Seville, Spain). This larger platform enabled data acquisition from all study sites in one single flight during the 2011 airborne campaigns, carrying both the micro-hyperspectral imager and a thermal camera concurrently.

Both UAV platforms were controlled by an autopilot for autonomous flying (AP04, UAV Navigation, Madrid, Spain) and followed a flight plan using waypoints to acquire imagery from all study fields (Fig. 1). The autopilot had a dual CPU controlling an integrated Attitude Heading Reference System (AHRS) based on a L1 GPS board, 3-axis accelerometers, gyros and a 3-axis magnetometer (Berni et al., 2009). The ground control station and the UAV were radio linked, transmitting position, attitude and status data at 20 Hz frequency; this tunneling transmission link was used for the operation of the hyperspectral imager from the ground station deployed near the study sites.

The hyperspectral imager carried by the UAVs in both 2010 and 2011 was a micro-hyperspectral camera (Micro-Hyperspec VNIR model, Headwall Photonics, MA, USA) in the spectral mode of 260 bands at 1.85 nm/pixel and 12-bit radiometric resolution. It yielded a FWHM of 3.2 nm with a 12-micron slit and 6.4 nm with a 25-micron slit in the 400–885 nm region. The 25-micron slit was selected in all flights of this study in order to increase the signal-to-noise ratio (SNR), as no

spectral binning was conducted when acquiring the imagery with the full bandset of 260 bands. Frame rate storage on board the UAV was set to 50 fps with an integration time of 18 ms. The 8-mm focal length lens yielded an IFOV of 0.93 mrad and an angular FOV of 50°, providing a swath of 522 m at 53 × 42 cm pixel resolution at 575 m AGL altitude and 75 km/h ground speed (Fig. 2a). The airborne campaigns conducted over the vineyard fields were flight lines in the solar plane at 9:00 am GMT in both 2010 and 2011. Each vineyard under study was targeted at the center of the flight lines. For identification purposes, each plot was marked in the field using ground control points detectable in the imagery. For each vineyard under study, spatial subsets were created (Fig. 2b;c) and subsequently used to extract image radiance.

The micro-hyperspectral sensor was radiometrically calibrated in the laboratory using derived coefficients with a calibrated uniform light source (integrating sphere, CSTM-USS-2000C Uniform Source System, LabSphere, NH, USA) at four levels of illumination and six integration times. Ortho-rectification of the hyperspectral imagery acquired with the UAV platforms was conducted using PARGE (ReSe Applications Schläpfer, Wil, Switzerland). This was done using input data acquired with a miniaturized inertial measuring unit (IMU) (MTiG model, Xsens, The Netherlands) installed on board and synchronized with the micro-hyperspectral imager (as in Zarco-Tejada
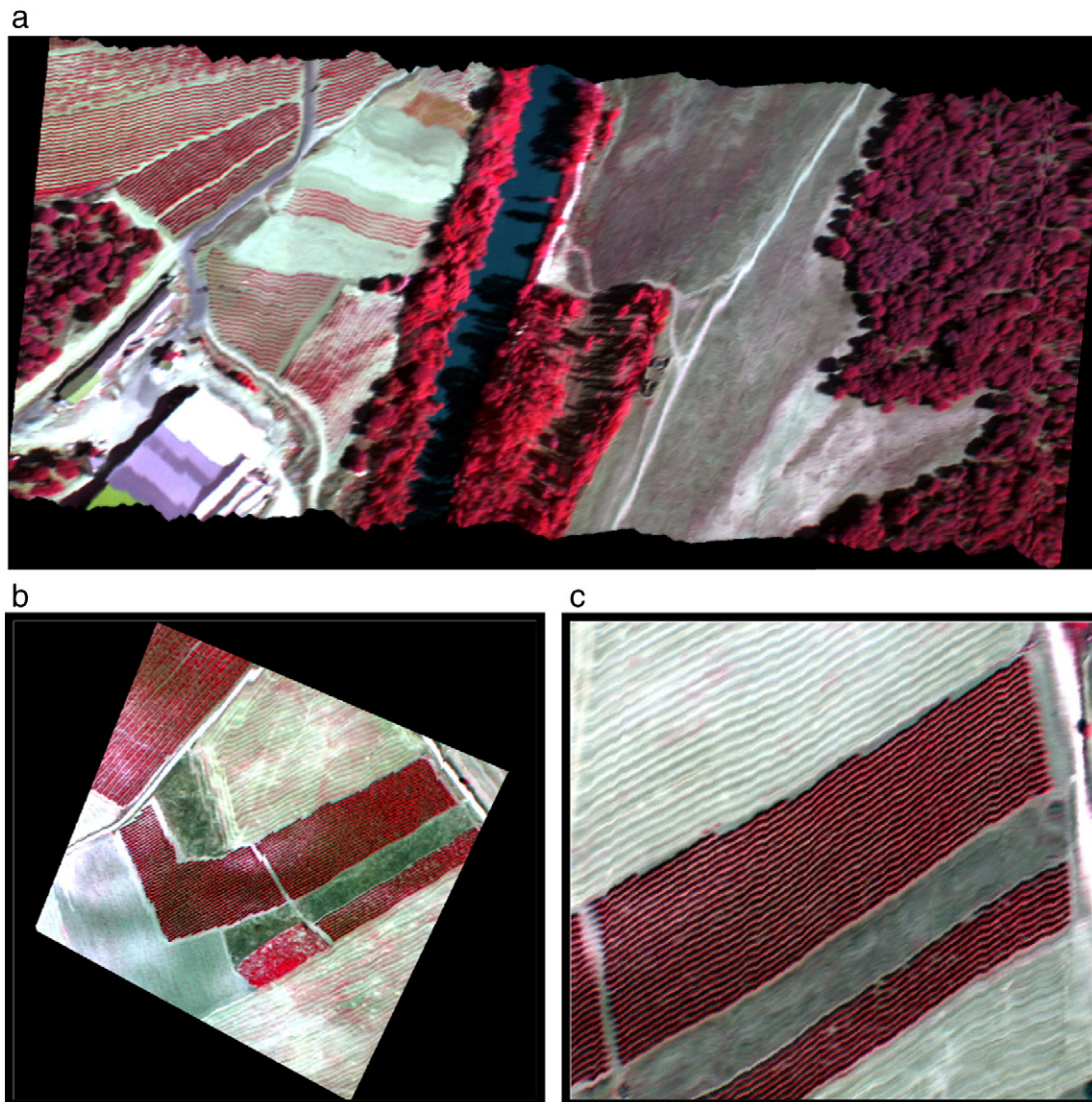

Fig. 2. Imagery acquired in the solar plane by the micro-hyperspectral sensor on board the unmanned aerial vehicle with an IFOV of 0.93 mrad and an angular FOV of 50º, yielding 53 × 42 cm pixel resolution at 575 m AGL altitude (a). Each vineyard under study was imaged at nadir (b), extracting the spectral radiance from each study plot (c).

et al., 2012). The hyperspectral imagery acquired enabled pure vine identification (Fig. 3a;b) using automatic object-based crown/vine detection algorithms. This methodology successfully separated vines from shaded and sunlit soil components in most cases, obtaining pure vine radiance without shadow and soil effects (Fig. 3c). Finally, mean radiance spectra were obtained for each study site (Fig. 4a). These radiance spectra were later used to calculate fluorescence retrieval at each study site using the O_2-A *in-filling* method. A total of 13 spectral bands were observed within the O_2-A feature with the airborne micro-hyperspectral imager (Fig. 4b).

2.2. Fluorescence retrieval method

Total incoming irradiance was measured at the time of the flights using a 0.065 nm full-width half-maximum (FWHM) Ocean Optics HR2000 fiber-optics spectrometer (Ocean Optics, Dunedin, FL, USA). The device was installed on a leveled pole with 2-m long, 600 μm optical fiber using a CC-3 VIS-NIR cosine corrector-diffuser (Ocean Optics, Dunedin, FL, USA). The 0.065 nm FWHM HR2000 spectrometer provided spectral measurements in the 680-770 nm range with 2048 channels. The spectrometer was specifically designed for fluorescence research targeting tree crowns in diurnal experiments, as described in Pérez-Priego et al. (2005). It had an H11 grating with 1800 lines/mm, a 5 μm slit, an L2 detector collection lens, an OF1-OG590 longpass filter and a set of high-reflectivity AgPlus mirrors model SAG-UPGD-HR to enhance the sensitivity of the instrument for high-resolution measurements in low light level experiments. Due to the dark current sensitivity of the instrument as a function of ambient temperature, a Peltier thermally insulated box model PT-100 (Magapor, Zaragoza, Spain) was used to house the spectrometer, keeping the internal temperature stable at 24 °C ± 1 °C during field measurements.

Irradiance (E) calibration of the spectrometer attached to the fiber with the cosine corrector-diffuser was conducted in the laboratory using a LS-1-CAL calibrated tungsten halogen NIST-traceable light source (Ocean Optics, Dunedin, FL, USA). To match the spectral resolution of the radiance imagery acquired by the hyperspectral airborne sensor, the high-resolution irradiance spectra measured with the HR2000 instrument was resampled through Gaussian convolution, observing the effects caused by the bandwidth on the depth in the O_2-A region (Fig. 5). Mean radiance spectra extracted from the airborne hyperspectral imagery at each study site for the 260 spectral bands were then used to estimate chlorophyll fluorescence. It should be noted that previous results obtained when retrieving the chlorophyll fluorescence signal using the micro-hyperspectral imager were characterized by a large spectral oversampling (1.85 nm sampling interval) and 6.4 nm bandwidths (Zarco-Tejada et al., 2012). Based on these data, the Fraunhofer Line Depth (FLD) principle calculated from a total of three bands for the *in* (L763 nm) and *out* bands (L750 nm; L780 nm) (FLD3) was applied to the hyperspectral imagery to quantify the fluorescence signal using the equations described in Zarco-Tejada et al. (2012). In particular, fluorescence (F) was quantified using the L_{in} (L763), L_{out} (average of L750 and L780 bands), E_{in} (E763), and E_{out} (average of E750 and E780 bands) (Fig. 6) using Eq. (1).

$$F = \frac{E_{out} \cdot L_{in} - E_{in} \cdot L_{out}}{E_{out} - E_{in}} \tag{1}$$

The FLD3 and other suitable methods for fluorescence estimation depending on the spectral data available (number of bands, spectral bandwidth available, signal-to-noise ratio of the instrument) can be reviewed in Meroni et al. (2010) and Damm et al. (2011). These studies, particularly those of Damm et al. (2011), proved in a simulation study
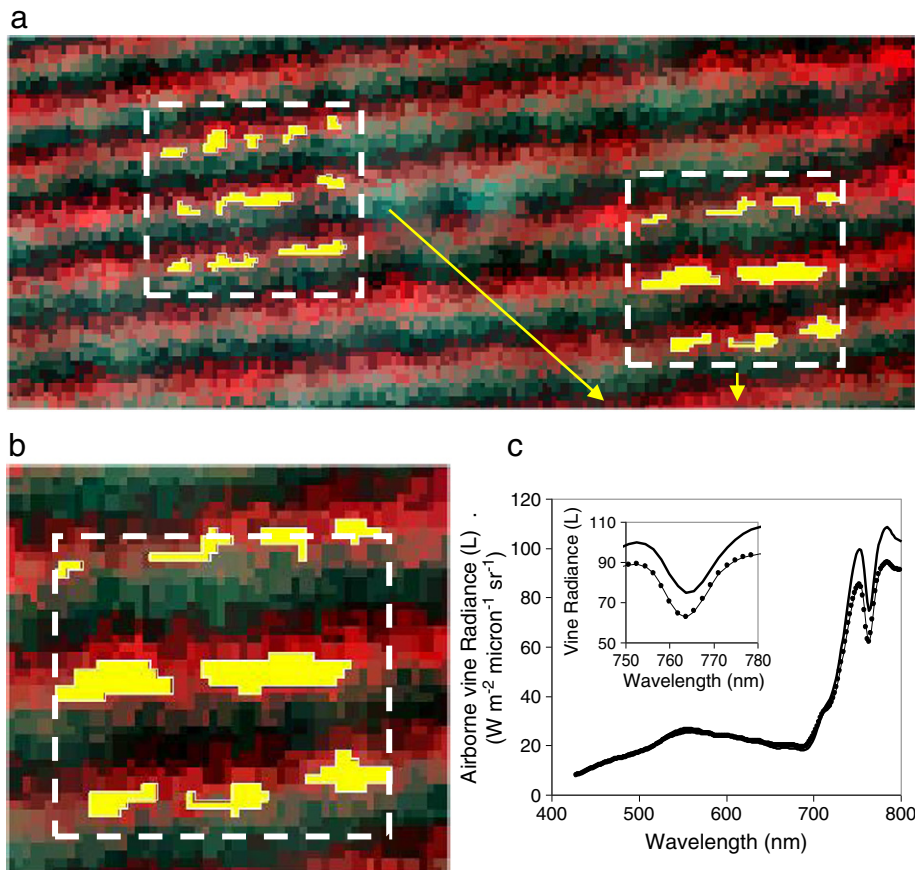

Fig. 3. Identification of pure vegetation pixels in each study plot from the airborne hyperspectral imagery using automatic object-based detection algorithms (a;b). Mean pure-vine radiance extracted from each site without shadow and soil effects (c).
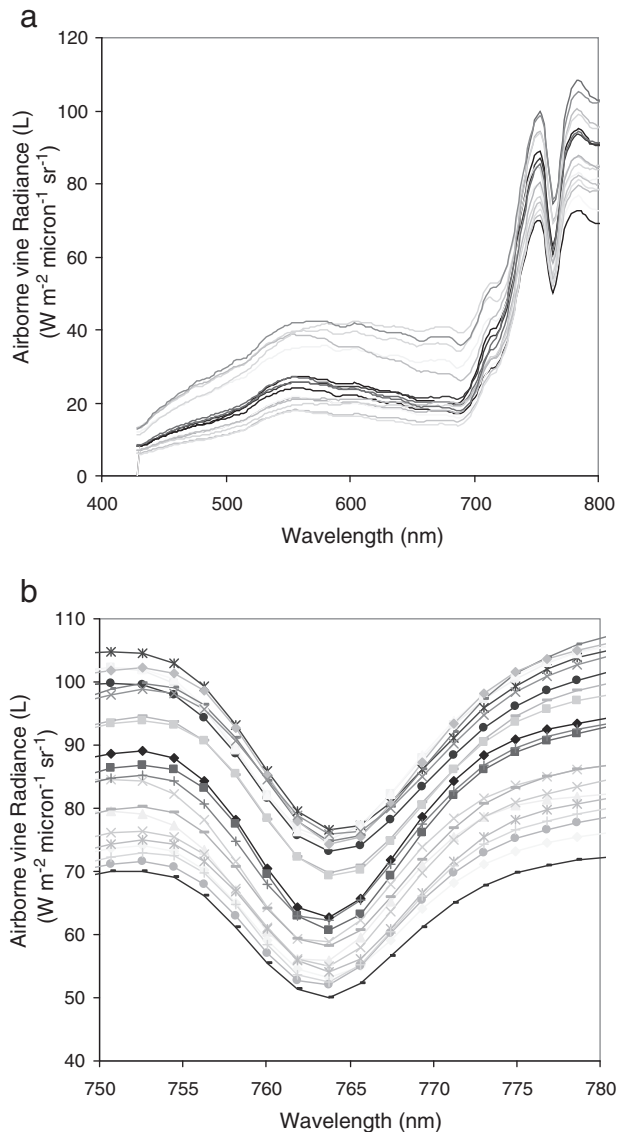
Fig. 4. Mean radiance spectra extracted from the airborne hyperspectral imagery collected from each study site at 260 bands, 1.85 nm/pixel, 12-bit radiometric resolution and 6.4 nm FWHM in the 400–885 nm region (a) showing the 13 spectral bands acquired within the O_2-A feature (b).

Fig. 5. Irradiance data acquired at the time of the airborne flights with the sub-nanometer HR2000 spectrometer in the 680-770 nm range (0.065 nm FWHM) and resampled through Gaussian convolution to match the FWHM of the airborne hyperspectral sensor.

3. Results

Relationships between leaf-level physiological measurements of net photosynthesis (P_n), stomatal conductance (G_s) and dark-adapted/ steady-state fluorescence parameters and leaf pigments at veraison are shown in Table 1 (year 2010) and Table 2 (year 2011). The two years yielded consistent significant results in both cases for the relationship between P_n and F_s ($r^2 = 0.55$; $p < 0.001$ for 2010; $r^2 = 0.59$; $p < 0.001$ for 2011) (Fig. 7a and b, respectively). Other fluorescence parameters that showed significant results (at $p < 0.01$ or $p < 0.001$ levels) for P_n were F_o', F_m' and NPQ. Consistently in both years, the best relationships with P_n were obtained for steady-state parameters such as F_o', F_m', F_v'/F_m' and F_s ($p < 0.001$), while the dark-adapted fluorescence parameters F_o, F_m, F_v and F_v/F_m yielded non-significant relationships ($p > 0.05$).

Relationships between G_s and P_n were significant in 2011 ($r = 0.56$; $p < 0.01$) but non-significant in 2010 ($r = 0.28$; $p > 0.05$). This result is probably due to higher water stress levels in 2011 as compared to 2010, which translated into a larger G_s and P_n gradient in 2011 (Table 3). This hypothesis is consistent considering the relationships

that the FLD3 method can retrieve the fluorescence signal when wider spectral bandwidths (i.e., 5 nm FWHM) are used along with high spectral sampling (below 2.5 nm) with instruments with a minimum of 300:1 signal-to-noise ratio. These modeling results agree with experimental fluorescence retrievals shown in Zarco-Tejada et al. (2012) obtained with the micro-hyperspectral imager used in the present manuscript. They are characterized by 260 bands acquired at 6.4 nm FWHM, 1.85 nm sampling interval (yielding a total of 13 spectral bands inside the O_2-A feature) and a signal-to-noise ratio of 300:1 without binning. Other FLD methods such as FLD, FLD2 and iFLD assessed in Zarco-Tejada et al. (2012) were not computed here as they yielded poorer results than the FLD3 method used with the Headwall Photonics VNIR micro-hyperspectral imager.

The airborne-derived fluorescence quantification for each year was compared with ground measurements of leaf-level fluorescence and net photosynthesis. Assessment of the relationships obtained for each independent year and both years together was conducted to determine whether the relationships found between airborne F and leaf P_n were statistically different.
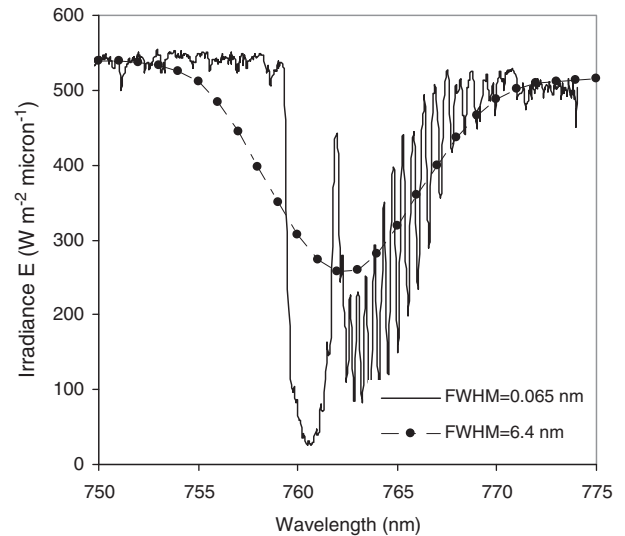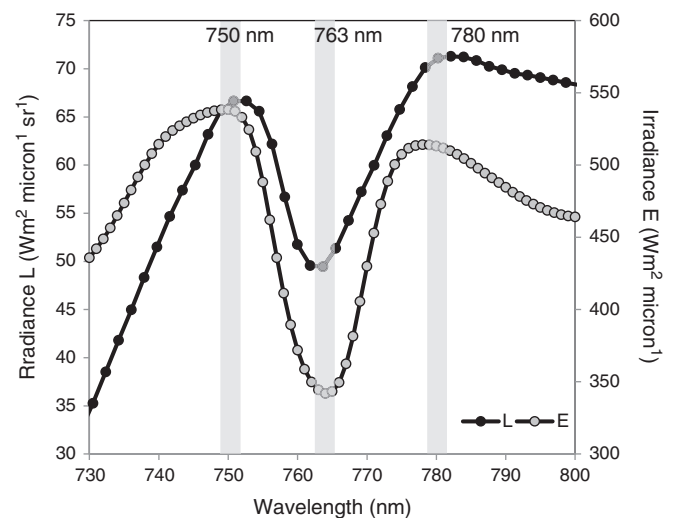

Fig. 6. Radiance (L) and irradiance (E) spectra showing the 750 and 780 nm (*out*) and 763 nm (*in*) bands used for fluorescence quantification through the FLD3 method.

Table 1

Relationships (Pearson correlation coefficient) between leaf-level physiological measurements of net photosynthesis (P_n), stomatal conductance (G_s) and dark-adapted (F_o, F_m, F_v, F_v/F_m) and steady-state fluorescence parameters (F_o', F_m', F_v'/F_m', F_s, $\Phi PSII$, qP, NPQ, ETR) and leaf pigments anthocyanins (Ant), chlorophyll $a + b$ (C_{ab}) and carotenoids (C_{xc}) acquired at veraison in 2010.

	Physiological measurements		Dark-adapted fluorescence				Steady-state fluorescence								Leaf pigments		
	P_n	G_s	F_o	F_m	F_v	F_v/F_m	F_o'	F_m'	F_v'/F_m'	F_s	$\Phi PSII$	qP	NPQ	ETR	Ant	C_{ab}	C_{xc}
P_n	1																
G_s	0.28	1															
F_o	−0.15	0.26	1														
F_m	0.00	−0.29	−0.11	1													
F_v	0.06	−0.33	−0.48*	0.93***	1												
F_v/F_m	0.10	−0.38	−0.88***	0.55**	0.82***	1											
F_o'	0.62**	0.19	−0.12	0.20	0.22	0.17	1										
F_m'	0.69***	0.27	−0.29	0.08	0.18	0.25	0.93***	1									
F_v'/F_m'	0.66***	0.36	−0.47*	−0.10	0.09	0.30	0.69***	0.89***	1								
F_s	0.74***	0.29	−0.26	0.08	0.17	0.22	0.94***	0.99***	0.86***	1							
$\Phi PSII$	0.16	−0.17	−0.58**	0.17	0.37	0.59**	0.11	0.28	0.47*	0.17	1						
qP	−0.23	−0.35	−0.18	0.23	0.27	0.31	−0.45*	−0.41*	−0.26	−0.51*	0.69***	1					
NPQ	−0.65***	−0.39	0.16	0.34	0.24	0.05	−0.81***	−0.89***	−0.85***	−0.88***	−0.18	0.48*	1				
ETR	0.17	−0.16	−0.59**	0.15	0.36	0.59**	0.07	0.25	0.46*	0.15	0.99***	0.71***	−0.15	1			
Ant	0.09	−0.05	−0.63**	0.18	0.40	0.62**	0.40	0.49*	0.56**	0.44*	0.70***	0.25	−0.39	0.69***	1		
C_{ab}	−0.02	−0.02	−0.61**	0.27	0.47*	0.63**	0.24	0.35	0.45*	0.29	0.65***	0.31	−0.18	0.66***	0.80***	1	
C_{xc}	0.18	−0.05	−0.56**	0.07	0.28	0.50*	0.42*	0.53**	0.53**	0.49*	0.52**	0.12	−0.41*	0.54**	0.68***	0.82***	1

* $p < 0.05$.
** $p < 0.01$.
*** $p < 0.001$.

Table 2

Relationships (Pearson correlation coefficient) between leaf-level physiological measurements of net photosynthesis (P_n), stomatal conductance (G_s) and dark-adapted (F_o, F_m, F_v, F_v/F_m) and steady-state fluorescence parameters (F_o', F_m', F_v'/F_m', F_s, $\Phi PSII$, qP, NPQ, ETR) and leaf pigments anthocyanins (Ant), chlorophyll $a + b$ (C_{ab}) and carotenoids (C_{xc}) acquired at veraison in 2011.

	Physiological measurements		Dark-adapted fluorescence				Steady-state fluorescence								Leaf pigments		
	P_n	G_s	F_o	F_m	F_v	F_v/F_m	F_o'	F_m'	F_v'/F_m'	F_s	$\Phi PSII$	qP	NPQ	ETR	Ant	C_{ab}	C_{xc}
P_n	1																
G_s	0.56**	1															
F_o	−0.24	0.00	1														
F_m	0.17	−0.06	−0.06	1													
F_v	0.20	−0.06	−0.21	0.99***	1												
F_v/F_m	0.34	−0.01	−0.54**	0.80***	0.86***	1											
F_o'	0.69***	0.46*	−0.34	0.54**	0.58**	0.64***	1										
F_m'	0.71***	0.52**	−0.48*	0.40*	0.46*	0.59**	0.92***	1									
F_v'/F_m'	0.48*	0.45*	−0.57**	0.14	0.22	0.41*	0.55**	0.81***	1								
F_s	0.76***	0.55**	−0.44*	0.39	0.44*	0.56**	0.92***	0.99***	0.79***	1							
$\Phi PSII$	0.20	−0.09	−0.48*	0.17	0.24	0.39	0.23	0.29	0.30	0.17	1						
qP	−0.21	−0.43*	0.05	0.06	0.05	0.02	−0.28	−0.40	−0.48*	−0.50*	0.67***	1					
NPQ	−0.66**	−0.58**	0.56**	0.09	0.01	−0.26	−0.72***	−0.87***	−0.81***	−0.86***	−0.26	0.45*	1				
ETR	0.21	−0.05	−0.47*	0.18	0.25	0.40*	0.26	0.32	0.32	0.19	0.99***	0.66***	−0.27	1			
Ant	0.60**	0.36	−0.34	0.47*	0.51*	0.48*	0.70***	0.76***	0.65***	0.74***	0.36	−0.16	−0.56**	0.39	1		
C_{ab}	0.32	0.16	−0.21	0.45*	0.47*	0.32	0.46*	0.51*	0.49*	0.47*	0.44*	0.03	−0.35	0.45*	0.79***	1	
C_{xc}	0.38	0.13	−0.35	0.42*	0.46*	0.38	0.51*	0.57**	0.54**	0.53**	0.46*	0.00	−0.44*	0.46*	0.82***	0.96***	1

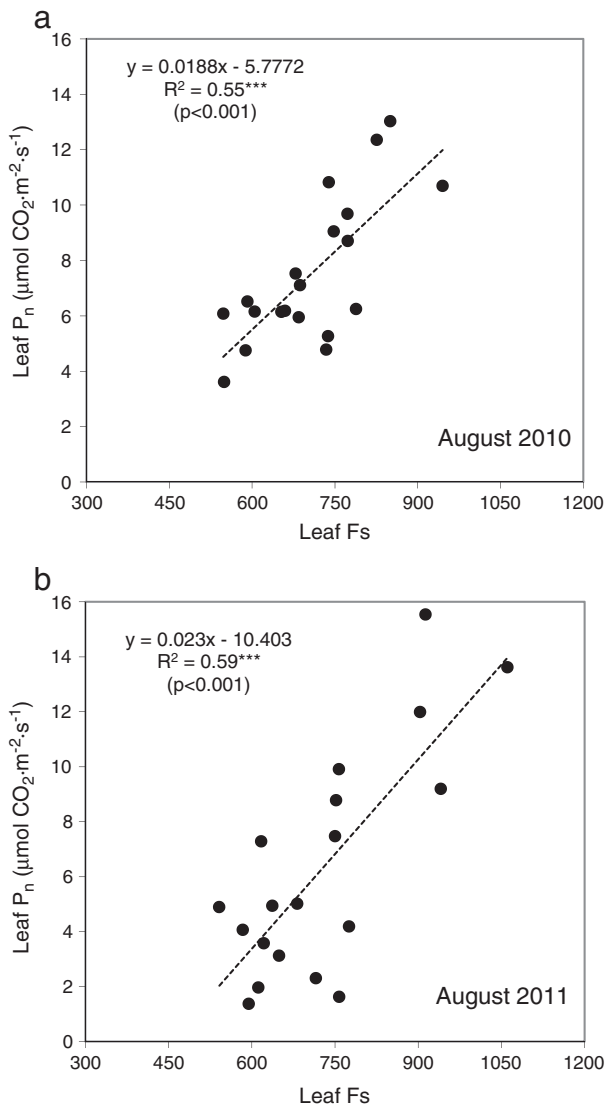* $p < 0.05$.
** $p < 0.01$.
*** $p < 0.001$.

Fig. 7. Leaf-level relationships obtained between net photosynthesis (P_n) and steady-state fluorescence (F_s) in 2010 (a) and 2011 (b).

obtained between G_s and fluorescence parameters, which were not significant in 2010 but showed significant values at 1% level in 2011 with F_m' (r = 0.52), F_s (r = 0.55) and NPQ (r = −0.58), and at 5% level with F_o', F_v'/F_m', and qP.

The analysis of the gradient of all parameters measured at leaf level at veraison in 2010 and 2011 (Table 3) showed that the P_n gradient was similar for 2010 and 2011 ($\mu = 7.53$ μmol CO_2 m^{-2} s^{-1} for 2010; $\mu = 6.35$ μmol CO_2 m^{-2} s^{-1} for 2011, with maximum recorded values of 13.03 μmol CO_2 m^{-2} s^{-1} for 2010 and 15.53 μmol

CO_2 m^{-2} s^{-1} for 2011). Nevertheless, G_s values clearly showed a wider gradient in 2011 when compared to 2010, with maximum values of 0.12 mol H_2O m^{-2} s^{-1} (2010) as compared to 0.21 mol H_2O m^{-2} s^{-1} (2011). Similar results were obtained for F_s measurements, which yielded similar values in both years ($\mu = 708.05$ for 2010; $\mu = 748.09$ for 2011) with maximum recorded values of 945.14 for 2010 and 1060.6 for 2011. The variability of the leaf pigment concentration data recorded showed a much higher gradient for 2011 than for 2010, with higher mean and maximum values recorded. The network of vineyard fields was selected because of its gradient in leaf nutrition levels, showing a great variability in leaf pigment values. However, no significant relationships were found between anthocyanins, chlorophyll $a + b$ and carotenes when compared against leaf P_n (except for Ant in 2011, $p < 0.01$) and leaf F_s. Consistently, probably due to the low gradient in water stress levels, G_s and leaf pigment content were not related (p was not significant in either year). As expected, relationships between Ant, C_{ab} and C_{xc} were highly significant in both years ($p < 0.001$), yielding correlation coefficients ranging from r = 0.68 to r = 0.96 in 2010 and 2011.

Mean leaf chlorophyll content per study site compared to leaf F_s (Fig. 8a;b) and P_n (Fig. 8c;d) for 2010 (Fig. 8a;c) and 2011 (Fig. 8b;d) showed that chlorophyll content estimation was not able to explain net photosynthesis levels under these conditions. While pigment content data were not significantly related to P_n levels in either year, steady-state fluorescence data measured at the leaf level yielded significant results (r = 0.74 & r = 0.76; $p < 0.001$; Tables 1 & 2). At the canopy image levels, the relationships obtained between mean leaf fluorescence per study site and fluorescence retrievals conducted from the airborne hyperspectral imagery using the FLD3 method yielded significant results for F_s ($r^2 = 0.48$; $p < 0.01$) (Fig. 9a) and F_v'/F_m' ($r^2 = 0.53$; $p < 0.01$) (Fig. 9b). These results show the agreement between the field-measured steady-state fluorescence F_s parameter (and F_v'/F_m') and airborne retrievals of F using the micro-hyperspectral imager.

The relationship between leaf P_n (mean calculated for each site) and airborne F (extracted from the imagery for each site) was consistent for both years separately, yielding significant relationships at $p < 0.01$ for 2010 ($r^2 = 0.54$) (Fig. 10a) and 2011 ($r^2 = 0.41$) (Fig. 10b) and a significant relationship at $p < 0.001$ for the aggregated years ($r^2 = 0.52$) (Fig. 10c). These results demonstrate that airborne F retrieval partially explained ($p < 0.001$) the P_n levels of the study sites imaged in 2010 and 2011. Statistical assessment was conducted with the Chow test (Chow, 1960), which explored whether the coefficients in the linear regressions were equal for years 2010 and 2011. The analysis did not find any differences between both samples (p-value = 0.75), that is, the coefficients in both linear regressions were equal for 2010 and 2011 and both years could be assessed together.

4. Discussion

Statistically significant relationships were obtained between airborne fluorescence quantified by the FLD3 method from hyperspectral

Table 3
Gradient analysis of the mean leaf physiological data of net photosynthesis (P_n, in μmol CO_2 m^{-2} s^{-1}), stomatal conductance (G_s, in mol H_2O m^{-2} s^{-1}), dark-adapted (F_o, F_m, F_v, F_v/F_m) and steady-state fluorescence parameters (F_o', F_m', F_v'/F_m', F_s, ΦPSII, qP, NPQ, ETR) and leaf anthocyanin (Ant), chlorophyll $a + b$ (C_{ab}) and carotenoid (C_{xc}) contents (μg cm^{-2}) acquired from the 24 study sites in 2010 and 2011.

|		Physiological measurements		Dark-adapted fluorescence				Steady-state fluorescence								Leaf pigments		
		P_n	G_s	F_o	F_m	F_v	F_v/F_m	F_o'	F_m'	F_v'/F_m'	F_s	ΦPSII	qP	NPQ	ETR	Ant	C_{ab}	C_{xc}
2010	Min	3.61	0.05	505.8	2054.9	1316	0.63	389.9	580.31	0.3	547.97	0.09	0.26	1.41	59.58	3.31	26.47	6.48
	Mean	7.53	0.0815	588.3	2501.6	1913.2	0.75	500.4	799.7	0.36	708.05	0.118	0.32	2.19	80.22	6.43	40.87	8.86
	Max	13.03	0.12	738.9	2786.7	2235.3	0.8	583.7	1046.4	0.42	945.14	0.15	0.41	3.32	101.15	8.79	52.79	11.68
2011	Min	1.37	0.05	439.27	1842.0	1357.7	0.72	406.47	620.04	0.29	541.54	0.09	0.24	1.37	63.3	5.40	36.97	8.26
	Mean	6.35	0.11	497.34	2639.7	2142.4	0.80	520.46	853.81	0.37	748.09	0.12	0.35	2.17	85.9	9.47	61.84	12.65
	Max	15.53	0.21	600.87	2882.8	2407.7	0.84	654.88	1180.2	0.47	1060.6	0.16	0.44	3	111.41	15.17	85.67	15.61
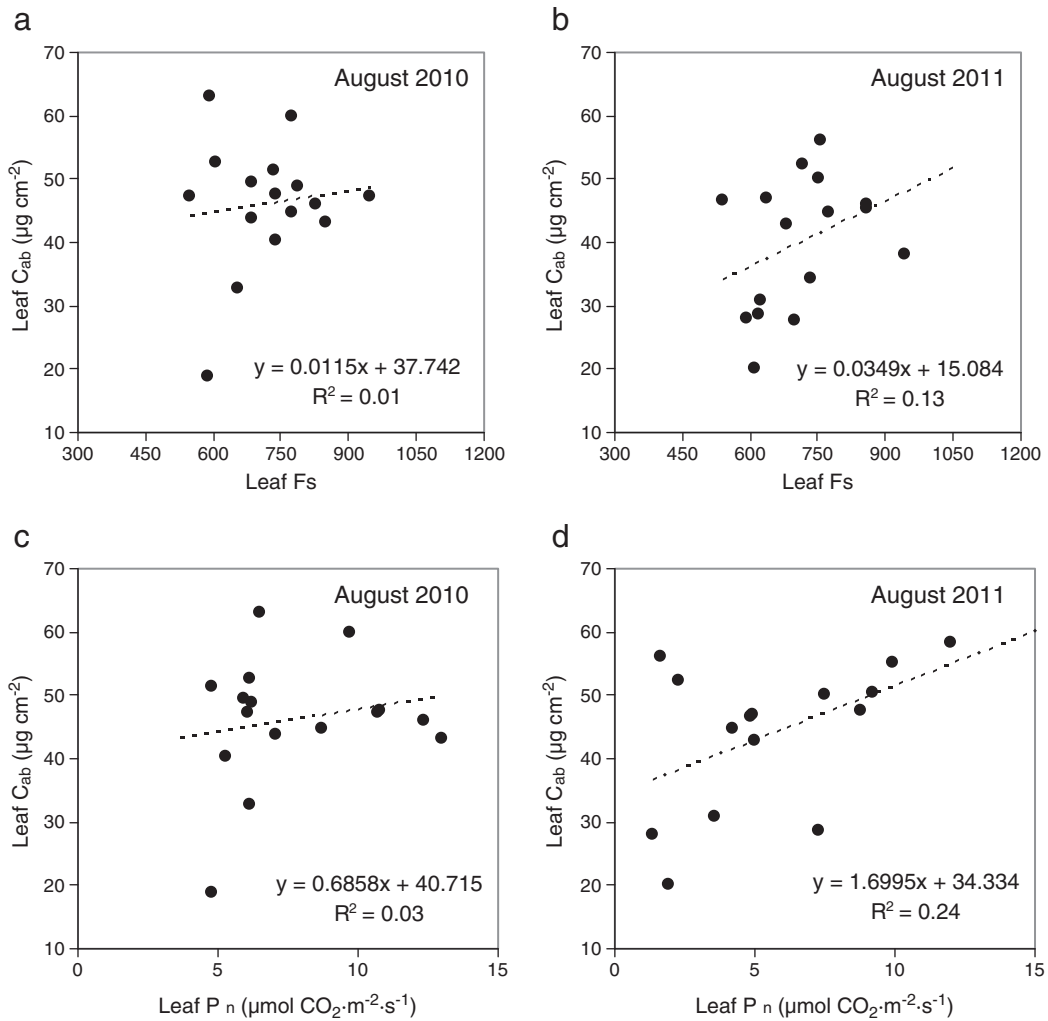
Fig. 8. Relationships obtained between mean leaf chlorophyll content per study site and leaf F_s (a;b) and P_n (c;d) in 2010 and 2011 at veraison, showing that chlorophyll concentration itself did not explain the P_n variability found within the sites studied.

imagery and field-measured net photosynthesis. These results were significant in two summer campaigns conducted in two consecutive years. These results represent progress in the efforts to assess the relationship between canopy fluorescence and photosynthesis, which was demonstrated in this study using very high resolution hyperspectral imagery. The hyperspectral imagery used in this study was characterized by coarse spectral resolution (i.e., 6.4 nm FWHM) and a narrow sampling interval (i.e., 1.85 nm). Nevertheless, the retrieval of fluorescence from measurements with such spectral resolution was possible for the conditions of this study area, characterized by flat areas with horizontally-homogeneous atmospheric conditions. This methodology is therefore ideal for precision agriculture and vegetation monitoring studies when using very high spatial resolution. An example of this is the physiological assessment of vegetation using airborne platforms or through close range plant phenotyping studies. Applying this methodology to densely vegetated areas or sites with topographic effects and/or highly loaded atmospheres (e.g., tropical rainforest) would require further assessments. Therefore, the methods presented in this study under such ideal conditions should be validated if applied to satellite imagery. In fact, modeling work should be conducted to assess the influence of such different environmental and atmospheric conditions on the quantification of fluorescence. As an example, the study by Damm et al. (2011) could be continued to account for atmospheric effects in their sensitivity analysis of F retrieval using the FLD method.

Another important issue that requires attention is the potential effect of photosystem I fluorescence in the 760 nm band. In fact, the relationship between chlorophyll fluorescence quantified at 760 nm and light use efficiency is being questioned by some authors (see the discussion in Porcar-Castell, 2012). These authors suggest that a large proportion of the fluorescence flux found at 760 nm is actually due to fluorescence emitted by photosystem I, mostly driven by chlorophyll absorption rather than by photosynthesis-related processes. Nevertheless, the results of the present study showed a weak correlation between chlorophyll content and fluorescence but a significant relationship between fluorescence at 760 nm and photosynthesis. In the two summer campaigns of the present study, the validation sites showed a range in leaf nutrition levels but a non-significant relationship ($p > 0.05$) between foliar anthocyanins, chlorophyll $a + b$ and carotenoid concentration when compared with leaf P_n and F_s. Therefore, the chlorophyll content variation did not explain the net photosynthesis variation under the conditions of this study. The lack of a relationship between P_n and C_{ab} in this study could be explained because in the study areas, i) net photosynthesis values were more strongly affected by changes in plant water status than by iron deficiency chlorosis (as shown in Tables 2 and 3), and ii) the predawn leaf water potential and stomatal conductance measurements used as indicators of plant water status were not significantly correlated with leaf chlorophyll content at veraison (G_c vs. C_{ab} were not related in either year, as shown in
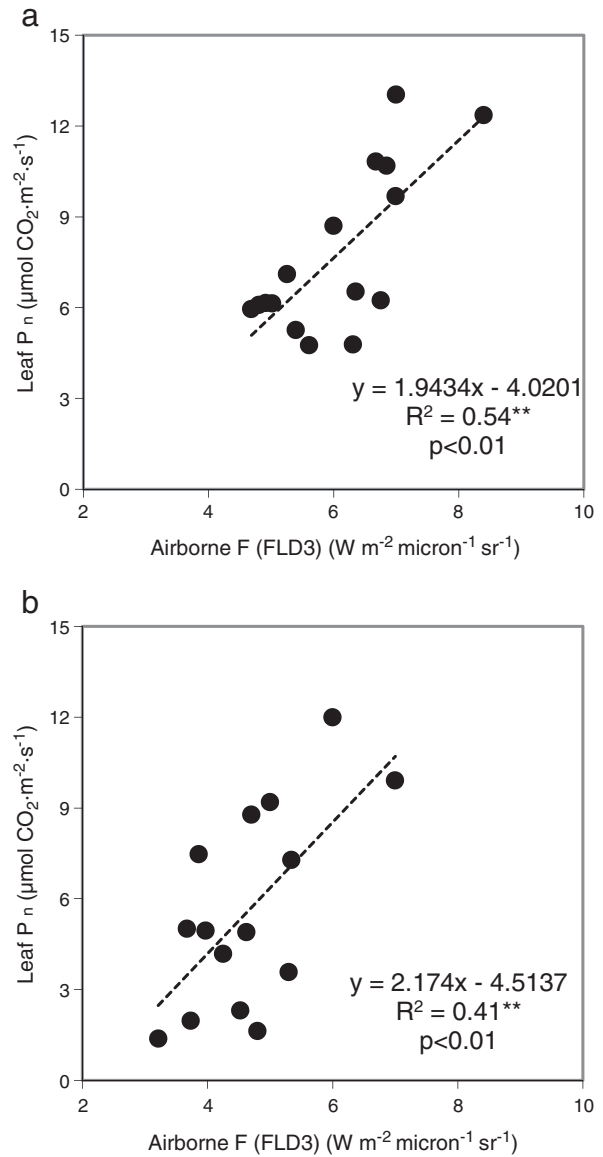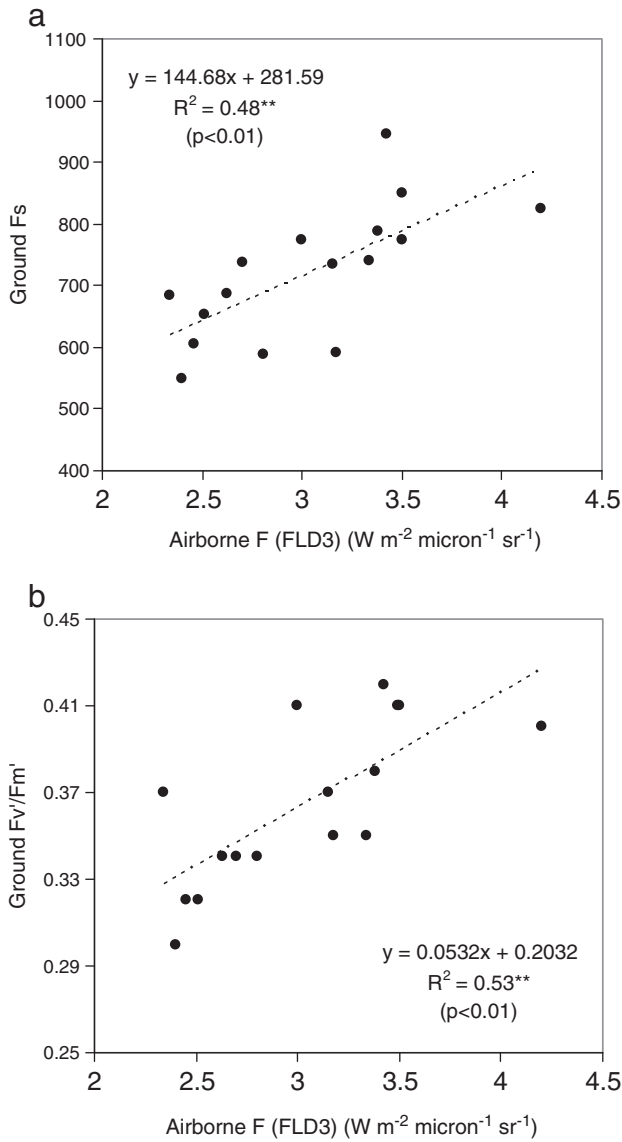
a

$$y = 144.68x + 281.59$$
$$R^2 = 0.48^{**}$$
$$(p<0.01)$$

Ground F_s

Airborne F (FLD3) (W m^{-2} micron^{-1} sr^{-1})

b

$$y = 0.0532x + 0.2032$$
$$R^2 = 0.53^{**}$$
$$(p<0.01)$$

Ground F_v'/F_m'

Airborne F (FLD3) (W m^{-2} micron^{-1} sr^{-1})

Fig. 9. Relationships obtained between mean leaf fluorescence per study site for F_s (a) and F_v'/F_m' (b) and fluorescence quantification using the FLD3 method from the airborne hyperspectral imagery.

Tables 2 and 3). In a study by Catalina et al. (2011), data from 2010 in the same study area showed separate interaction effects of both water status and nutritional levels on vine vigor, yield and most composition parameters. Thus, fluorescence could be a good estimator of net photosynthesis levels in vineyards affected by water deficit (Flexas et al., 1998, 2000), but also in those in which water and nutritional stress are present simultaneously. This issue is critical and requires further studies conducted with pure vegetation pixels extracted from high-resolution imagery before global fluorescence maps derived from GOSAT-FTS data in 760 nm and other future platforms can be interpreted.

Another important issue that needs further development is the interpretation of the fluorescence signal from large pixels where all scene components are mixed. Specifically, pixel-aggregation effects at such coarse spatial resolutions need to be accounted for to fully understand the fluorescence retrieved from large pixels with different levels of fractional cover, background effects, vegetation densities and photosynthetic pigment absorption levels. An initial attempt was recently made to understand the effects of fractional cover on the retrieval of airborne fluorescence quantified from aggregated pixels, using both leaf/canopy fluorescence models linked to a geometric

a

Leaf P_n (μmol $CO_2 \cdot m^{-2} \cdot s^{-1}$)

$$y = 1.9434x - 4.0201$$
$$R^2 = 0.54^{**}$$
$$p<0.01$$

Airborne F (FLD3) (W m^{-2} micron^{-1} sr^{-1})

b

Leaf P_n (μmol $CO_2 \cdot m^{-2} \cdot s^{-1}$)

$$y = 2.174x - 4.5137$$
$$R^2 = 0.41^{**}$$
$$p<0.01$$

Airborne F (FLD3) (W m^{-2} micron^{-1} sr^{-1})

c

Leaf P_n (μmol $CO_2 \cdot m^{-2} \cdot s^{-1}$)

$$y = 1.872x - 3.3536$$
$$R^2 = 0.52^{***}$$
$$p<0.001$$

Airborne F (FLD3) (W m^{-2} micron^{-1} sr^{-1})

Fig. 10. Relationships obtained between leaf P_n and airborne F in 2010 (a), 2011 (b) and the aggregated 2010 + 2011 years (c).

model. The FluorFLIM model developed was used to retrieve pure tree crown fluorescence from aggregated pixels using very high resolution hyperspectral imagery (Zarco-Tejada et al., 2013). The conclusions of that study suggested that without proper modeling work to account for such spatial variability of the fractional cover, global maps of fluorescence would look very similar to standard NDVI maps due to the large effects of the fractional cover on both NDVI and fluorescence retrieved from large pixels.

Finally, it is important to highlight the difficulties of validating fluorescence retrieval methods conducted with high-resolution imagery at global scales. The main sources of complexity lie in the temporal and spatial variability of within-canopy leaf physiological status as regards both assimilation rates and fluorescence measures, which require several measurements acquired concurrently. It is extremely challenging to conduct validation work in such complex and heterogeneous canopies, especially if a number of study sites are required to provide a range of physiological conditions. In a study such as ours, measurements collected from several study sites within the time of the airborne flights posed additional difficulties due to the diurnal variation of both fluorescence and assimilation rates. Moreover, although this study was conducted on flat areas and it was possible to identify the study sites well, there were several challenges. Such difficulties were related to atmospheric effects, imagery calibration, methodological aspects of the quantification of the fluorescence signal from pure vegetation pixels extracted with little background and shade mixture effects, and complex operational aspects regarding the operation of the micro-hyperspectral imager on board an unmanned aerial vehicle. Even under these challenging methodological, technical and field experimental and sampling conditions, results of this study of two-year campaigns showed statistically significant relationships, with p-values < 0.01 in most cases, and with $p < 0.001$ for the P_n vs. airborne F_s relationship for the two years/campaigns of study. Further validation studies such as the one described here are needed to better understand the validity of modeling results developed and reported for ideal simulation conditions, which in most cases do not face the challenges described when complex fieldwork is required. Without proper validation studies to report conclusions on the relationships between field-based and airborne/satellite retrieved fluorescence conducted under varying physiological conditions, species, and canopy architectures, progress on fluorescence retrieval science will be limited to modeling efforts. These simulation methods are of critical importance. Yet, they are currently limited to the existing simulation models available, which in most cases do not entirely mimic the conditions of the real heterogeneous and complex cropping and natural vegetation systems. The lack of a linked leaf-canopy radiative transfer model to simulate fluorescence emission in heterogeneous canopies is a clear example of the current limitations of fluorescence quantification efforts on the modeling front.

5. Conclusions

The study presented in this manuscript assessed the relationships between chlorophyll fluorescence measures and net photosynthesis acquired at the leaf and canopy levels. High-resolution airborne imagery with 40 cm resolution and 260 spectral bands in the 400–885 nm spectral region was used. It was acquired from a micro-hyperspectral sensor and enabled the identification of pure vegetation pixels. During two summers, radiance spectra were extracted from validation sites where steady-state and dark-adapted fluorescence measurements were conducted as well as data on photosynthesis and stomatal conductance. Leaf pigment concentration such as chlorophyll content, carotenoids and anthocyanin concentration were also measured from the validation sites and the relationships between pigment content and photosynthesis levels were explored. The Fraunhofer Line Depth (FLD) principle using a total of three bands (FLD3) for the *in* (L763 nm) and *out* bands (L750 nm; L780 nm) (FLD3) was applied to the hyperspectral imagery to estimate the fluorescence signal.

Results obtained between leaf-level net photosynthesis and fluorescence parameters yielded significant results: $r^2 = 0.55$ ($p < 0.001$) for 2010 and $r^2 = 0.59$ ($p < 0.001$) for 2011. Fluorescence parameters such as F_o', F_m' and NPQ also were significant when compared to leaf P_n. Consistently in both years, the best relationships with P_n were obtained for steady-state parameters such as F_o', F_m', F_v'/F_m' and F_s ($p < 0.001$). Although the validation sites showed a range in leaf nutrition levels, no significant relationships ($p > 0.05$) were found between foliar anthocyanins, chlorophyll $a + b$ and carotenoid concentration when compared with leaf P_n and F_s. Moreover, the chlorophyll content variation itself did not explain the net photosynthesis variation under the conditions of this study. Such results were due to the varying effects of both photosynthetic pigment content and plant water status levels found on the study sites. In this study, net photosynthesis was more affected by changes in plant water status than by iron deficiency chlorosis. This indicated that stomatal conductance as indicator of plant water status was not significantly correlated with leaf chlorophyll content. Under these conditions, a relationship was observed between leaf F_s and net photosynthesis for both field campaigns conducted in 2010 and 2011.

The retrieval of the fluorescence signal from the airborne hyperspectral imagery through the FLD3 method yielded significant results when compared with ground truth F_s ($r^2 = 0.48$; $p < 0.01$). This confirms the feasibility of F retrieval using the airborne micro-hyperspectral imager. The link between leaf P_n and airborne F was proven in the two years of the experiment, yielding significant relationships ($r^2 = 0.52$, $p < 0.001$). These results provide insight on efforts to monitor photosynthesis through fluorescence emission quantification using remote sensing imagery. A critical aspect is that fluorescence quantification was conducted in pure vegetation pixels, therefore removing most of the effects of the structure, shadows and the background on hyperspectral radiance data.

Acknowledgments

References

Berni, J. A. J., Zarco-Tejada, P. J., Suárez, L., & Fereres, E. (2009). Thermal and narrow-band multispectral remote sensing for vegetation monitoring from an unmanned aerial vehicle. *IEEE Transactions on Geoscience and Remote Sensing, 47*(3), 722–738.

Catalina, A., González, R., González, M. R., Zarco-Tejada, P. J., & Martín, P. (2011). Iron and water stress differently affect vine photosynthetic efficiency and grape composition. *Proc. XXXIV World Congress of Vine and Wine, 20-27th June, Porto, Portugal.*

Chow, G. C. (1960). Tests of equality between sets of coefficients in two linear regressions. *Econometrica, 28*(3), 591–605.

Damm, A., Elbers, J., Erler, E., Gioli, B., Hamdi, K., Hutjes, R., et al. (2010). Remote sensing of sun induced fluorescence to improve modeling of diurnal courses of gross primary production (GPP). *Global Change Biology, 16*, 171–186.

Damm, A., Erler, A., Hillen, W., Meroni, M., Schaepman, M. E., Verhoef, W., et al. (2011). Modeling the impact of spectral sensor configurations on the FLD retrieval accuracy of sun-induced chlorophyll fluorescence. *Remote Sensing of Environment, 115*, 1882–1892.

Dobrowski, S. Z., Pushnik, J. C., Zarco-Tejada, P. J., & Ustin, S. L. (2005). Simple reflectance indices track heat and water stress-induced changes in steady-state chlorophyll fluorescence at the canopy scale. *Remote Sensing of Environment, 97*, 403–414.

Escalona, J. M., Flexas, J., & Medrano, H. (1999). Stomatal and non-stomatal limitations of photosynthesis under water stress in field-grown grapevines. *Australian Journal of Plant Physiology, 26*, 421–433.

Evain, S., Flexas, J., & Moya, I. (2004). A new instrument for passive remote sensing: 2. Measurement of leaf and canopy reflectance changes at 531 nm and their relationship with photosynthesis and chlorophyll fluorescence. *Remote Sensing of Environment, 91*, 175–185.

Flexas, J., Briantais, J. M., Cerovic, Z., Medrano, H., & Moya, I. (2000). Steady–state and maximum chlorophyll fluorescence responses to water stress in grapevine leaves: a new remote sensing system. *Remote Sensing of Environment, 73*, 282–297.

Flexas, J., Escalona, J. M., & Medrano, H. (1998). Down-regulation of photosynthesis by drought under field condition in grapevine leaves. *Australian Journal of Plant Physiology, 25*, 893–900.

Frankenberg, C., Fisher, J. B., Worden, J., Badgley, G., Saatchi, S. S., Lee, J. -E., et al. (2011). New global observations of the terrestrial carbon cycle from GOSAT: Patterns of plant fluorescence with gross primary productivity. *Geophysical Research Letters, 38*, L17706. http://dx.doi.org/10.1029/2011GL048738.

Gamon, J. A., Peñuelas, J., & Field, C. B. (1992). A narrow-wave band spectral index that tracks diurnal changes in photosynthetic efficiency. *Remote Sensing of Environment, 41*, 35–44.

González, R., Núñez, L. C., Martín, P., Berjón, A., & Zarco-Tejada, P. J. (2005). Estimación de la absorbancia de radiación PAR en hojas de vid a partir de su contenido en clorofila. *V Congreso Ibérico de Ciencias Hortícolas*, Actas Portuguesas de Horticultura, Vol. 2, Asociación Portuguesa de CC. Hortícolas (Ed.), Lisboa, (pp. 384–389). Oporto. Portugal, 22–27 May 2005.

Grace, J., Nichol, C., Disney, M., Lewis, P., Quaife, T., & Bowyer, P. (2007). Can we measure terrestrial photosynthesis from space directly, using spectral reflectance and fluorescence? *Global Change Biology, 13*, 1484–1497.

Guanter, L., Frankenberg, C., Dudhia, A., Lewis, P. E., Gomez-Dans, J., Kuze, A., et al. (2012). Retrieval and global assessment of terrestrial chlorophyll fluorescence from GOSAT space measurements. *Remote Sensing of Environment, 121*, 236–251.

Joiner, J., Yoshida, Y., Vasilkov, A. P., Yoshida, Y., Corp, L. A., & Middleton, E. M. (2011). First observations of global and seasonal terrestrial chlorophyll fluorescence from space. *Biogeosciences, 8*(3), 637–651.

Krause, G. H., & Weis, E. (1984). Chlorophyll fluorescence as a tool in plant physiology. II. Interpretation of fluorescence signals. *Photosynthesis Research, 5*, 139–157.

Kuze, A., Suto, H., Nakajima, M., & Hamazaki, T. (2009). Thermal and near infrared sensor for carbon observation Fourier-transform spectrometer on the Greenhouse Gases Observing Satellite for greenhouse gases monitoring. *Applied Optics, 48*, 6716–6733.

Larcher, W. (1994). Photosynthesis as a tool for indicating temperature stress events. In E. D. Schulze, & M. M. Caldwell (Eds.), *Ecophysiology of Photosynthesis* (pp. 261–277). Berlin: Springer.

Lichtenthaler, H. K. (1987). Chlorophylls and carotenoids: Pigments of photosynthetic biomembranes. In L. Parker, & R. Douce (Eds.), *Plant cell membranes. Methods in enzymology, Vol. 148*. (pp. 350–383). New York: Academic Press.

Lichtenthaler, H. K. (1992). The Kautsky effect: 60 years of chlorophyll fluorescence induction kinetics. *Photosynthetica, 27*, 45–55.

Lichtenthaler, H. K., & Rinderle, U. (1988). The role of chlorophyll fluorescence in the detection of stress conditions in plants. *CRC Critical Reviews in Analytical Chemistry, 19*(Suppl. 1), S29–S85.

Louis, J., Ounis, A., Ducruet, J. M., Evain, S., Laurila, T., Thum, T., et al. (2005). Remote sensing of sunlight-induced chlorophyll fluorescence and reflectance of Scots pine in the boreal forest during spring recovery. *Remote Sensing of Environment, 96*, 37–48.

Malenovsky, Z., Mishra, K. B., Zemek, F., Rascher, U., & Nebal, L. (2009). Scientific and technical challenges in remote sensing of plant canopy reflectance and fluorescence. *Journal of Experimental Botany, 60*, 2987–3000.

Meroni, M., Busetto, L., Colombo, R., Guanter, L., Moreno, J., & Verhoef, W. (2010). Performance of spectral fitting methods for vegetation fluorescence quantification. *Remote Sensing of Environment, 114*, 363–374.

Meroni, M., Colombo, R., & Cogliati, S. (2004). High resolution leaf spectral signature for the detection of solar induced chlorophyll fluorescence. *Proceedings of the 2nd International Workshop on Remote Sensing of Solar Induced Vegetation Fluorescence, Montreal, Canada, 17–19 November 2004*.

Meroni, M., Picchi, V., Rossini, M., Cogliati, S., Panigada, C., Nali, C., et al. (2008a). Leaf level early assessment of ozone injuries by passive fluorescence and PRI. *International Journal of Remote Sensing, 29*(17), 5409–5422.

Meroni, M., Rossini, M., Guanter, L., Alonso, L., Rascher, U., & Colombo, R. (2009). Remote sensing of solar-induced chlorophyll fluorescence: Review of methods and applications. *Remote Sensing of Environment, 113*, 2037–2051.

Meroni, M., Rossini, M., Picchi, V., Panigada, C., Cogliati, S., Nali, C., et al. (2008b). Assessing steady-state fluorescence and PRI from hyperspectral proximal sensing as early indicators of plant stress: The case of ozone exposure. *Sensors, 8*, 1740–1754.

Miller, J. R., Berger, M., Alonso, L., Cerovic, Z., Goulas, Y., Jacquemoud, S., et al. (2004). Progress on the development of an integrated canopy fluorescence model, 2003. *International Geoscience and Remote Sensing Symposium, IGARSS'03, Vol. 1*. (pp. 601–603). Toulouse, France: Institute of Electrical and Electronics Engineers Inc. (IEEE) (21–25/7/2004. ISBN 0-7803-7929-2 - 0-7803-7930-6).

Moya, I., Camenen, L., Evain, S., Goulas, Y., Cerovic, Z. G., & Latouche, G. (2004). A new instrument for passive remote sensing 1. Measurements of sunlight-induced chlorophyll fluorescence. *Remote Sensing of Environment, 91*, 186–197.

Naumann, J. C., Young, D. R., & Anderson, J. E. (2007). Linking leaf chlorophyll fluorescence properties to physiological responses for detection of salt and drought stress in coastal plant species. *Physiologia Plantarum, 131*, 422–433.

Naumann, J. C., Young, D. R., & Anderson, J. E. (2008). Leaf chlorophyll fluorescence, reflectance, and physiological response to freshwater and saltwater flooding in the evergreen shrub, *Myrica cerifera. Environmental and Experimental Botany, 63*, 402–409.

Nichol, C. J., Rascher, U., Matsubara, S., & Osmond, B. (2006). Assessing photosynthetic efficiency in an experimental mangrove canopy using remote sensing and chlorophyll fluorescence. *Trees, 20*, 9–15.

Papageorgiou, G. (1975). Chlorophyll fluorescence: An intrinsic probe of photosynthesis. In Govindjee (Ed.), *Bioenergetics of photosynthesis* (pp. 319–371). New York: Academic Press.

Pedrós, R., Goulas, Y., Jacquemoud, S., Louis, J., & Moya, I. (2010). FluorMODleaf: A new leaf fluorescence emission model based on the PROSPECT model. *Remote Sensing of Environment, 114*, 155–167.

Pedrós, R., Jacquemoud, S., Goulas, Y., Louis, J., & Moya, I. (2004). A new leaf fluorescence model. *2nd International Workshop on Remote Sensing of Solar Induced Vegetation Fluorescence, 17–19 November. Canada: Montreal*.

Pedrós, R., Moya, I., Goulas, Y., & Jacquemoud, S. (2008). Chlorophyll fluorescence emission spectrum inside a leaf. *Photochemical and Photobiological Sciences, 7*(4), 498–502.

Pérez-Priego, O., Zarco-Tejada, P. J., Sepulcre-Cantó, G., Miller, J. R., & Fereres, E. (2005). Detection of water stress in orchard trees with a high-resolution spectrometer through chlorophyll fluorescence in-filling of the O2-A band. *IEEE Transactions on Geoscience and Remote Sensing, 43*, 2860–2869.

Porcar-Castell, A. (2012). Interactive comment on "Chlorophyll fluorescence remote sensing from space in scattering atmospheres: implications for its retrieval and interferences with atmospheric CO2 retrievals" by C. Frankenberg et al. *Atmos. Meas. Tech. Discuss., 5*. (pp. C969–C971).

Rascher, U., Agati, G., Alonso, L., Cecchi, G., Champagne, S., Colombo, R., et al. (2009). CEFLES2: The remote sensing component to quantify photosynthetic efficiency from the leaf to the region by measuring sun-induced fluorescence in the oxygen absorption bands. *Biogeosciences Discussions, 6*(7), 2217–2266.

Rascher, U., & Pieruschka, R. (2008). Spatio-temporal variations of photosynthesis—The potential of optical remote sensing to better understand and scale light use efficiency and stresses of plant ecosystems. *Precision Agriculture, 9*, 355–366.

Schreiber, U., & Bilger, W. (1987). Rapid assessment of stress effects on plant leaves by chlorophyll fluorescence measurements. In J. D. Tenhunen, & E. M. Catarino (Eds.), *Plant Response to Stress* (pp. 27–53). Berlin, Germany: Springer-Verlag.

Schreiber, U., Bilger, W., & Neubauer, C. (1994). Chlorophyll fluorescence as a nonintrusive indicator for rapid assessment of in vivo photosynthesis. In E. D. Schulze, & M. M. Caldwell (Eds.), *Ecophysiology of photosynthesis. Ecological studies, Vol. 100*. (pp. 49–70). Berlin Heidelberg New York: Springer.

Steele, M., Gitelson, A., Rundquist, D., & Merzlyak, M. (2009). Nondestructive estimation of anthocyanin content in grapevine leaves. *American Journal of Enology and Viticulture, 60*(1), 87–92.

Strack, D., & Wray, V. (1989). Anthocyanins. In J. B. Harborne (Ed.), *Plant phenolics. Methods in Plant Biology, Vol. 1*. (pp. 325–356). London, UK: Academic Press/Harcourt Brace Jovanovich.

Stylinski, C. D., Gamon, J. A., & Oechel, W. C. (2002). Seasonal patterns of reflectance indices, carotenoid pigments and photosynthesis of evergreen chaparral species. *Oecologia, 131*, 366–374.

Suárez, L., Zarco-Tejada, P. J., Berni, J. A. J., González-Dugo, V., & Fereres, E. (2009). Modelling PRI for water stress detection using radiative transfer models. *Remote Sensing of Environment, 113*, 730–744.

Suárez, L., Zarco-Tejada, P. J., Sepulcre-Cantó, G., Pérez-Priego, O., Miller, J. R., Jiménez-Muñoz, J. C., et al. (2008). Assessing canopy PRI for water stress detection with diurnal airborne imagery. *Remote Sensing of Environment, 112*, 560–575.

Van der Tol, C., Verhoef, W., & Rosema, A. (2009a). A model for chlorophyll fluorescence and photosynthesis at leaf scale. *Agricultural and Forest Meteorology, 149*(1), 96–105.

Van der Tol, C., Verhoef, W., Timmermans, J., Verhoef, A., & Su, Z. (2009b). An integrated model of soil-canopy spectral radiances, photosynthesis, fluorescence, temperature and energy balance. *Biogeosciences, 6*, 3109–3129.

Verhoef, W. (2004). Extension of SAIL to model solar-induced canopy fluorescence spectra. *2nd International Workshop on Remote Sensing of Solar Induced Vegetation Fluorescence, 17–19 Nov. Canada: Montreal*.

Zarco-Tejada, P. J., Berjón, A., López, R., Miller, J. R., Martín, P., & González, M. R. (2005). Assessing vineyard condition with hyperspectral indices: Leaf and canopy reflectance simulation in a row-structured discontinuous canopy. *Remote Sensing of Environment, 99*, 271–287.

Zarco-Tejada, P. J., Berni, J. A. J., Suárez, L., & Fereres, E. (2008). A new era in remote sensing of crops with unmanned robots. *SPIE Newsroom*. http://dx.doi.org/10.1117/2.1200812.1438.

Zarco-Tejada, P. J., Berni, J. A. J., Suárez, L., Sepulcre-Cantó, G., Morales, F., & Miller, J. R. (2009). Imaging chlorophyll fluorescence from an airborne narrow-band multi-spectral camera for vegetation stress detection. *Remote Sensing of Environment, 113*, 1262–1275.

Zarco-Tejada, P. J., González Dugo, V., & Berni, J. A. J. (2012). Fluorescence, temperature and narrowband indices acquired from a UAV platform for water stress detection using a micro-hyperspectral imager and a thermal camera. *Remote Sensing of Environment, 117*, 322–337.

Zarco-Tejada, P. J., Suarez, L., & Gonzalez-Dugo, V. (2013). Spatial resolution effects on chlorophyll fluorescence retrieval in a heterogeneous canopy using hyperspectral imagery and radiative transfer simulation. *Geoscience and Remote Sensing Letters, IEEE, 9*. http://dx.doi.org/10.1109/LGRS.2013.2252877.